How to cite: *Angew. Chem. Int. Ed.* **2021**, *60*, 10716–10723
International Edition: doi.org/10.1002/anie.202016768
German Edition: doi.org/10.1002/ange.202016768

Bioinorganic Chemistry

Re^{I} Tricarbonyl Complexes as Coordinate Covalent Inhibitors for the SARS-CoV-2 Main Cysteine Protease

*Johannes Karges, Mark Kalaj, Milan Gembicky, and Seth M. Cohen**

Abstract: *Since its outbreak, the severe acute respiratory syndrome—coronavirus 2 (SARS-CoV-2) has impacted the quality of life and cost hundreds-of-thousands of lives worldwide. Based on its global spread and mortality, there is an urgent need for novel treatments which can combat this disease. To date, the 3-chymotrypsin-like protease ($3CL^{pro}$), which is also known as the main protease, is considered among the most important pharmacological targets. The vast majority of investigated $3CL^{pro}$ inhibitors are organic, non-covalent binders. Herein, the use of inorganic, coordinate covalent binders is proposed that can attenuate the activity of the protease. Re^{I} tricarbonyl complexes were identified that demonstrate coordinate covalent enzymatic inhibition of $3CL^{pro}$. Preliminary studies indicate the selective inhibition of $3CL^{pro}$ over several human proteases. This study presents the first example of metal complexes as inhibitors for the $3CL^{pro}$ cysteine protease.*

Introduction

Since its outbreak in December 2019 in Wuhan (Hubei, China), the severe acute respiratory syndrome—coronavirus 2 (SARS-CoV-2) has spread across the world. On 11th March, the World Health Organization (WHO) officially declared this pulmonary disease as a global pandemic. To date, more than 96 million cases have been reported with more than 2 million confirmed deaths,[1] creating an urgent need for the development of novel therapeutics.

The papain-like protease (PL^{pro}) and the 3-chymotrypsin-like protease ($3CL^{pro}$), which is also known as the main protease, are considered among the most important viral targets for SARS-CoV-2. Clinical studies have indicated that infected patients treated with protease inhibitors have shown reduced symptoms and mortality.[2] The PL^{pro} and $3CL^{pro}$ proteases are responsible for the processing of the viral polyproteins pp. 1a and pp. 1b that mediate functions required for viral replication and transcription and are crucial for viral maturation and infectivity.[3,4] The inhibition of these proteases significantly disrupt the viral life cycle, presenting an important opportunity for therapeutic intervention.[5] The compound disulfiram, which is approved for chronic alcohol dependence, has been reported to inhibit the PL^{pro} protease of SARS and is currently under investigation for SARS-CoV-2.[6] Recently, the use of Au complexes as potential therapeutics has been reported, including as PL^{pro} inhibitors.[7,8] As inhibitors of the $3CL^{pro}$ protease, the approved HIV therapeutics Lopinavir and Ritonavir are being studied in Phase III clinical trials for SARS-CoV-2.[9] In addition, a number of other organic compounds are under consideration in preclinical trials as inhibitors of these proteases.[10–13] Among these compounds, a handful of inhibitors have been identified that covalently bind to the catalytically active Cys145 amino acid.[13–15] Despite these contributions, irreversible Michael acceptors such as Rupintrivir have failed in clinical trials due to their low bioavailability,[16] in part due to reactions with off-target biological thiols. To address this limitation, the generation of reversible Cys-binding inhibitors has received increased attention in order to better target the Cys145 residue in the $3CL^{pro}$ protease active site.[17]

Metal-based coordination compounds can exhibit sophisticated 3-dimensional (3D) shapes[18–24] and can be designed to have selective reactivity, providing a pathway to develop covalent enzyme inhibitors.[25–27] In this context, the use of 3D metal complexes as potential coordinate covalent inhibitors for the SARS-CoV-2 main protease $3CL^{pro}$ is presented. A $[Re(2,2'\text{-bipyridine})(CO)_3]^+$ fragment was identified that could bind to the catalytically active Cys145 amino acid through a metal-cysteine bond. The 2,2′-bipyridine ligand of the fragment was derivatized with various functional groups and chloride and water axial capping ligands were examined to develop a rudimentary structure–activity relationship (SAR). The resulting complexes were synthesized, characterized, and their in vitro activity investigated. To the best of our knowledge, these are the first metal complexes reported as inhibitors for the SARS-CoV-2 main protease $3CL^{pro}$.

Results and Discussion

Rational Design

Previous studies by Fricker and co-workers demonstrated that Au^{III}, Pd^{II}, and Re^{V} complexes can inhibit the activity of the cysteine proteases Cathepsin B and K. These studies indicated that metal complexes can interact with catalytically active cysteine residues upon release of monodentate ligands to form coordinate covalent, but reversible, adducts.[28,29] These studies provided the motivation to examine a variety of metal complexes for activity against $3CL^{pro}$. Complexes of Pb, Bi, Te, Ni, Cu, Zn, Ru, Rh, Pd, Ag, Cd, Re, Pt, Au, and Hg were considered due to their high metal–sulfur bond enthalpy, especially in comparison to their metal-oxygen or metal-

[*] Dr. J. Karges, M. Kalaj, Dr. M. Gembicky, Prof. S. M. Cohen
Department of Chemistry and Biochemistry
University of California, San Diego
La Jolla, CA 92093 (USA)
E-mail: scohen@ucsd.edu
Supporting information and the ORCID identification number(s) for the author(s) of this article can be found under: https://doi.org/10.1002/anie.202016768.

nitrogen bond enthalpy, which would be expected to produce high thiophilicity for Cys residues over other amino acid residues.[30,31] Coordination compounds of these metals that were generally associated with poorer biological compatibility were removed from further consideration, resulting in compounds based on Ru, Rh, Pd, Re, Pt, or Au as possible options. Subsequently, known classes of compounds (Figure S1) possessing one vacant coordination site to allow for a metal–Cys bond were then modelled inside the active site pocket of $3CL^{pro}$.

The molecular geometry of potential candidates (Figure S1) was determined using density-functional theory (DFT) calculations; each candidate possessed a chlorine atom as a placeholder for the enzyme coordination site. The geometry of the calculated structures was verified by comparison with crystal structures of structurally related compounds from the Cambridge Crystallographic Data Centre (CCDC). For docking experiments, the chlorine atom was removed to yield the "active" fragment for enzyme binding which was further considered as a rigid body. The metal complex was then docked to the Cys residues found in $3CL^{pro}$. The enzyme possesses 12 Cys residues (Cys16, Cys22, Cys38, Cys44, Cys85, Cys117, Cys128, Cys145, Cys156, Cys160, Cys65, Cys300); however, the majority of these are buried inside the protein, with only three Cys (Cys85, Cys145, Cys156) surface accessible to fragments. After coordinating covalent docking of the complexes to these Cys residues, the binding pose was energetically minimized and scored using the GBVI/WSA dG force fields provided by MOE.

Among the modelled compounds, the *fac*-$Re(CO)_3(NN)$ (NN = bidentate nitrogen-donating ligand) fragment stood out as an attractive candidate (Table S1) that matched the protein architecture and could potentially react with the Cys145 active site residue (Figure 1, Figure S2). Among the docked binding poses, the fragment with the lowest energy was found to coordinate to Cys145 and not the other surface Cys residues. Previous studies have discussed the application of Re^{I} tricarbonyl as anticancer agents, luminescent probes, or radio-imaging agents, suggesting the biocompatibility of such compounds.[32–37] Additional docking studies were performed with the scaffold that possessed symmetric substituents in all positions of the 2,2′-bipyridine ligand (vide infra). The docking pose of the Re^{I} tricarbonyl complexes functionalized with polar groups demonstrated opportunities to interact with the protein active site by hydrogen bonding and hydrophobic interactions. With these docking studies in hand, a series of complexes with either chloride or water as a labile ligand were synthesized, characterized, and evaluated as $3CL^{pro}$ inhibitors.

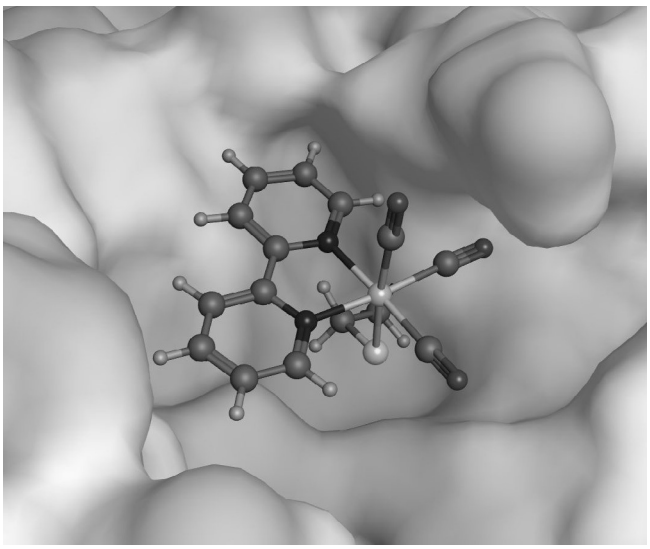

Figure 1. Docking pose of the $[Re(2,2'\text{-bipyridine})(CO)_3]^+$ fragment bound to the thiol of Cys145 in the active site of $3CL^{pro}$.

Synthesis and Characterization

The synthesis of complexes **1**, **3**–**7**, **10**–**12**, **17**–**18**, **20**, **22**, **27**, and **32** have been previously described (see Supporting Information for details), while **2**, **8**–**9**, **13**–**16**, **19**, **21**, **23**–**26**, **28**–**31**, and **33**–**42** have not been previously reported (Figure 2). The functionalized 2,2′-bipyridine derivatives were prepared via literature procedures (see Supporting Information for details). The chloride capped Re^{I} tricarbonyl complexes **1**–**21** were synthesized by complexation of pentacarbonylchlororhenium with the corresponding 2,2′-bipyridine ligand. The aqua Re^{I} tricarbonyl complexes **22**–**42** were prepared by treatment of the chloride coordinated complex with silver trifluoromethanesulfonate, followed by precipitation upon addition of water. The aqua complexes were found

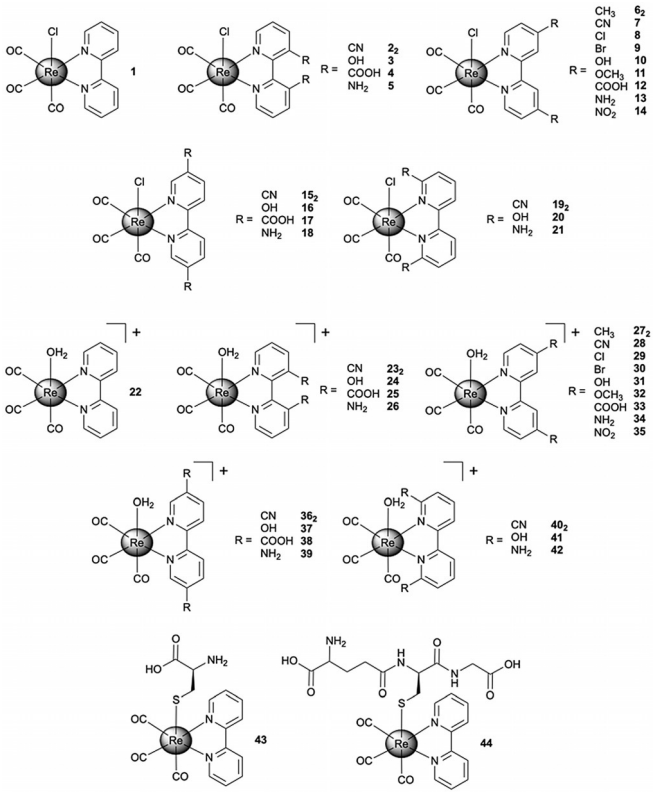

Figure 2. Chemical structure of Re^{I} tricarbonyl complexes investigated in this study. The aqua coordinated complexes were isolated as triflate salts.

to generally have higher aqueous solubility then the corresponding chloride coordinated complexes. The identity of the resulting compounds was verified by NMR spectroscopy and high-resolution mass spectrometry (HRMS). The purity of all compounds was confirmed by HPLC analysis (Figure S3–S7).

The molecular structure of several Re^{I} tricarbonyl complexes was determined by single-crystal X-ray diffraction. The structures **1**,[38,39] **6**,[40] **7**,[41,42] **10**,[43] **11**,[40] **17**,[44] **18**,[45] **20**,[46] **27**,[47] and **32**[47] have already been reported. The structures of compounds, **3**, **8**, **13**, **14**, **15**, **19**, **22**, **37**, and **42** are reported here (Figure 3, Table S2–S4). Although the structures of compounds **7**, **11**, and **20** have been reported elsewhere (as mentioned above), new structures of these compounds were obtained that possess different cell parameters reflective of solvent molecules used during the crystallization process. All of the structures show that a central Re^{I} ion is bound to the bipyridine in a bidentate fashion, with the remaining Re^{I} coordination sphere occupied by three carbonyl ligands and an axial chloride ion or water molecule. In the water bound complexes, triflate anions charge balance the overall monocationic charge of the complex. Interestingly, compound **3** is the first 3,3′-disubstituted 2,2′-bipyridine crystal structure using this Re^{I} based scaffold and the bulkiness of the adjacent hydroxyl groups in the 3-position resulted in distortion of the typically planar aromatic bipyridine rings to an out-of-plane motif. Moreover, the distorted planar angle resulting from steric bulk is also noteworthy in compounds **19** and **42** with 6,6′-subsituted bipyridine ligands (Figure S8). In compound **19** the N_1-Re_1-Cl_1 bond angle is 82.22(7)° and in compound **42** the N_1-Re_1-O_1 bond angle is 79.52(12)° with deviations of 7.88° and 10.48° degrees from complete planarity (see Supporting Information for details). For several of the studies described below, the Re^{I} tricarbonyl complexes with the unsubstituted 2,2′-bipyridine ligand (chloride **1** and water **22** coordinated) were used as model compounds for each respective groups of compounds.

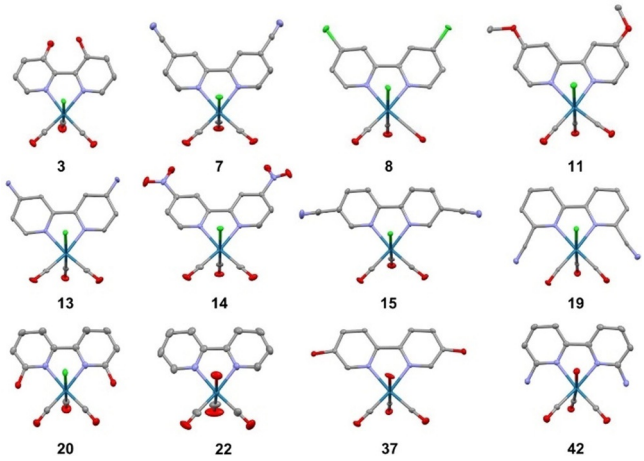

Figure 3. X-ray crystal structures of Re^{I} complexes **3**, **7**, **8**, **11**, **13**, **14**, **15**, **19**, **20**, **22**, **37**, and **42** (50% probability ellipsoids). Solvent, anions, and hydrogen atoms have been omitted for clarity.[57]

Stability

The stability of these compounds is an essential parameter for application as an enzyme inhibitor.[48] Representative complexes **1** and **22** were incubated in water or phosphate buffered saline (PBS) at 37 °C for 24 h in the dark and then analysed by HPLC. Compound **22** did not show any changes over the course of this experiment, while **1** showed slow hydrolysis of the chloride ligand, to yield complex **22** (Figures S9, S10). No other degradation products of these compounds were observed over this time period, suggesting that only the hydration of the chloride complex **1** needs to be considered in the context of the other experiments described herein.

Reactivity with Amino Acids

The interaction of the chloride (**1**) and aqua (**22**) Re^{I} tricarbonyl complex with amino acids containing cationic (N_α-*p*-tosyl-L-arginine methyl ester, L-histidine methyl ester, L-lysine methyl ester), anionic (N_α-*tert*-butoxycarbonyl-L-aspartic acid *tert*-butyl ester), polar (L-serine methyl ester, L-asparagine *tert*-butyl ester), and sulphur (L-cysteine methyl ester, L-methionine methyl ester) side chains was investigated (Figure 4) using equimolar amounts of metal complex and amino acid. Previous studies have indicated that Re^{I} tricarbonyl complexes are able to react with Cys derivatives[47,49,50] and a crystal structure has revealed that the Cys is covalently bound in axial position.[49]

The Re^{I} tricarbonyl complexes **1** and **22** were incubated in water at 37 °C with the corresponding amino acid for 24 h and analysed by HPLC. While **1** did not react with the majority of amino acids, it did react with L-cysteine methyl ester, presumably due to the high thiophilicity of the Re^{I} centre. In contrast, **22** showed reactivity toward the acidic N_α-*tert*-butoxycarbonyl-L-aspartic acid *tert*-butyl ester and the basic L-histidine methyl ester amino acids, but did not achieve full conversion over 24 h. Notably, the incubation of **22** with L-cysteine methyl ester resulted in a single product peak with full conversion within 24 h. For additional insight into the kinetics of the capping group, the hydrolysis of the chloride ligand was investigated upon incubation of **1** in water and determination of the amount of hydrolysed product by HPLC in a time-dependent manner. Based on this experiment, the difference in reactivity between **1** and **22** can be explained by the slow hydrolysis rate of the chloride ligand in **1** with a value of $0.355 \pm 0.051 \times 10^{-3}\ s^{-1}$. Following this evaluation, the crude product of the incubation of **22** with L-cysteine methyl ester was analysed by ESI-MS confirming the generation of [Re(2,2′-bipyridine)(L-cysteine methyl ester)$(CO)_3$] ($[M+H]^+$ calcd for $C_{17}H_{17}N_3O_5ReS$: 562.0, found: 562.4). These results suggest that these compounds could serve as coordinate covalent inhibitors by binding to the catalytically active Cys145 in $3CL^{pro}$.

Following this assessment, the reaction of **22** with L-cysteine methyl ester was further investigated. Using the carbonyl signals in the IR spectrum, the change of the coordination sphere of the Re^{I} complex can be used to

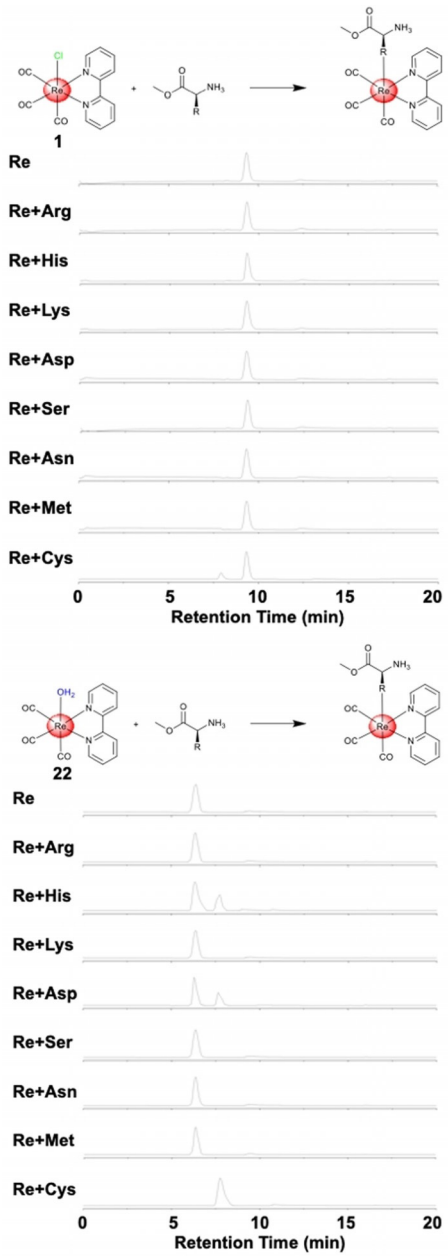

Figure 4. HPLC traces of the chloride **1** (top) and aqua **22** (bottom) Re^{I} tricarbonyl complexes after exposure to amino acids for 24 h.

monitor its reactivity (Figure S11). As expected, the carbonyl signals from the starting material **22** (2047, 1935, 1905 cm^{-1}) to [Re(2,2′-bipyridine)(L-cysteine methyl ester)$(CO)_3$] (2050, 1930, 1900 cm^{-1}) are shifted. Furthermore, additional peaks for the methyl ester (1719 cm^{-1}) and the broad amine signal (2940 cm^{-1}) stemming from the amino acid also appear. This interaction was also investigated by using UV/Vis absorption spectroscopy (Figure S11). Compound **22** and L-cysteine methyl ester were mixed and the absorption spectrum was collected every 2 min for 120 min. The absorption spectrum shows immediate changes and within 30 min forms a new spectrum with the appearance of two isosbestic points, indicating a clean transformation of **22** to the Cys adduct. After 60 min, no further changes in the absorption spectrum was observed. The interaction of **22** with L-cysteine methyl ester was also investigated by ^{1}H NMR spectroscopy (Figure S11). Immediately after mixing of the two starting materials (≈5 min), a new set of signals was observed indicative of the formation of [Re(2,2′-bipyridine)(L-cysteine methyl ester)$(CO)_3$]. While the aromatic protons of the bipyridine ligand were shifted high field, the β-CH_2 of the cysteine side chain and α-CH protons were shifted slightly low field. Within 60 min, the signals for **22** completely disappeared, suggesting a full conversion to the amino acid metal complex.

The relatively rapid reactivity of **22** with thiol-containing molecules could be potentially problematic due to the high concentration of glutathione in cells. The axial functionalized Cys (**43**) and glutathione (**44**) derivatives were synthesized by mixing of the corresponding thiol with **22** in water overnight (see Supporting Information for details). To study the reversibility of this reaction, **43** was incubated with equimolar amounts of glutathione and **44** with Cys at 37 °C. After 24 h, the generated products were analysed by HPLC. The bound thiol was exchanged in both cases, showing the reversibility of this reaction (Figure S12) and therefore the possibility of the Re^{I} tricarbonyl complex to interact with Cys145 in $3CL^{pro}$ despite the presence of other reactive biological thiols.

Biochemical Evaluation

After confirmation of the ability of the Re^{I} tricarbonyl complexes to coordinate covalently bind to Cys derivatives, the binding to the SARS-CoV-2 $3CL^{pro}$ was investigated using ESI-TOF MS.[51] While the native protein was found to have a deconvoluted mass of 33797 (Figure S13), upon incubation with **22** for 2 h the mass shifted to 34225 (Figure S14), corresponding to a single attached Re^{I} tricarbonyl complex (*m*/*z* 427). To investigate if the metal complex was bound to the predicted cysteine residue, $3CL^{pro}$ was first incubated with the well-characterized inhibitor GC376, which covalently binds to Cys145 as confirmed by macromolecular X-ray crystallography.[14] As expected, GC376 formed a new species (*m*/*z* 34201) with a mass difference of *m*/*z* 404, corresponding to the correct mass for the GC376-protein covalent adduct (Figure S15). Incubation of $3CL^{pro}$ with GC376, followed by incubation with **22** resulted in only the formation of the GC376-protein covalent adduct (*m*/*z* 34201), with no mixture of adducts and no addition of the Re^{I} tricarbonyl complex (Figure S16). These results strongly suggest that **22** is targeting the same residue as GC376, namely active site Cys145.

Following this initial assessment, the inhibition activity against the SARS-CoV-2 $3CL^{pro}$ was investigated. The $3CL^{pro}$ protease was pre-incubated with Re^{I} compounds and enzyme inhibition was monitored by conversion of a non-fluorescent substrate to a fluorescent product (see Supporting Information for details). Compounds **1**–**42** were screened against $3CL^{pro}$ at a concentration of 200 μM (Figure 5). As expected, due to the slow release of the chloride atom, compounds **1**–**21** did not show significant inhibition activity. In contrast, all aqua compounds **22**–**42** were able to inhibit the activity of the protease, with remaining enzymatic activity reduced to ≈20–

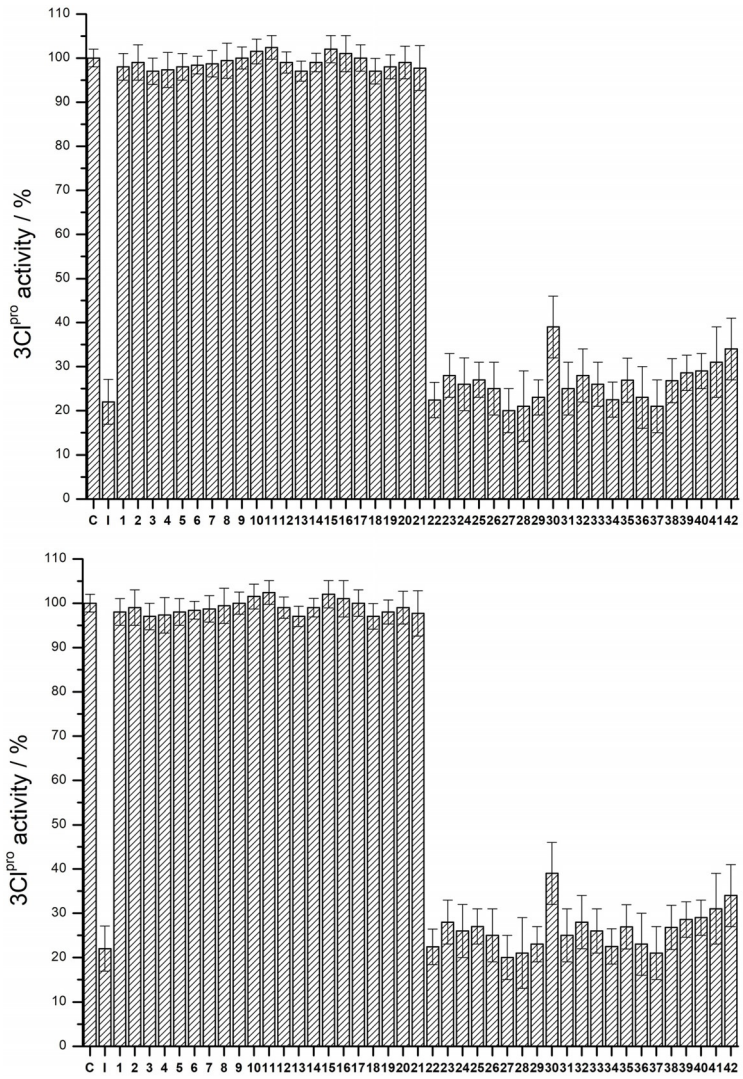

Figure 5. Enzyme activity assay of 3CL^{pro} with **1**–**42** (C = control, no inhibitor; I = known covalent inhibitor GC376) at a concentration of: 200 μM (*top*) or 50 μM (*bottom*). Values and error bars are derived from three independent experiments.

40 %. The aqua compounds were subsequently screened against 3CL^{pro} at a lower concentration of 50 μM (Figure 5). Interestingly, the 4,4′- (**27**–**35**) and 5,5′- (**36**–**39**) substituted complexes generally displayed stronger inhibitory activity when compared to the 3,3′- (**22**–**26**) and 6,6′- (**40**–**42**) substituted complexes. However, none of the compounds displayed significantly greater activity than the unsubstituted parent compound **22**. Overall, compounds **22**, **31**–**34**, **37**–**39** were identified as having the strongest inhibitory effect and were therefore studied further.

The inhibition by the lead structures was quantified by determination of their IC_{50} values (Table 1). The complexes displayed IC_{50} values between 7.5–24.1 μM (Figure S17). The carboxylic acid functionalized compounds (**33**, **38**) have the highest IC_{50} values while the amine functionalized compounds (**34**, **39**) have the lowest IC_{50} values. This could be the result of these functional groups being directed at negatively charged surfaces inside the enzyme active site (Figure S18). Based on this hypothesis, the carboxylic acids on the Re^{I} tricarbonyl complex would result in a repulsion with the protein surface, while the amine substituents would present attractive interactions, resulting in the observed differences in inhibition activity. Although only a preliminary SAR, the observation that preferred substitution patterns and functional groups on the bipyridine group can be identified suggests that more selective and active Re^{I} compounds can be designed for inhibition of 3CL^{pro}. Overall, **34** was identified as having the

Table 1: Summary of the binding data of selected compounds against 3CL^{pro}. Values and standard deviations are derived from three independent experiments.

Compound	IC_{50} [μM]
22	13.8 ± 2.1
31	12.8 ± 1.9
32	15.7 ± 1.4
33	24.1 ± 1.2
34	7.5 ± 1.3
37	13.5 ± 2.3
38	21.1 ± 2.7
39	9.6 ± 1.3

lowest IC_{50} value at 7.5 ± 1.3 μM. To ensure that the intact coordination compound **34** is responsible for the inhibitory effect, the ligand 4,4′-diamino-2,2′-bipyridine and the metal complex pentacarbonylchlororhenium were screened against $3CL^{pro}$. Both components showed no activity (IC_{50} value > 100 μM), confirming that **34** is the active species.

As glutathione and other biologically present thiols in cells could influence the activity of these compounds, the activity of the Cys **43** and glutathione **44** functionalized derivatives towards $3CL^{pro}$ was tested. The complexes were found to display slightly mitigated activity compared to many of the aqua complexes (**43**, $IC_{50} = 20.8 \pm 3.6$ μM; **44**, $IC_{50} = 26.7 \pm 4.1$ μM). A hallmark of covalent inhibitors is time-dependent inhibition; therefore, **1** (axial Cl), **22** (axial H_2O), **43** (axial Cys), and **44** (axial glutathione) derivatives (at a concentration of 20 μM) were pre-incubated with $3CL^{pro}$ for various time periods (30, 60, 120, and 240 min) and the remaining enzyme activity was measured (Figure S19). While **1** demonstrated no inhibition and **22** showed near complete inhibition over this time period, **43** and **44** showed a gradual reduction of $3CL^{pro}$ activity as a function of time. Within 240 min, **43** and **44** had reduced enzymatic activity to the same level as compound **22**, indicating that these axial thiols can be exchanged, acting as reversible, coordinate covalent inhibitors. Such thiol substituted Re^{I} tricarbonyl complexes could even serve as a type of prodrug for this class of coordinate covalent inhibitors.

To further examine the effect of glutathione on inhibitory activity, an enzyme inhibition assay with compound **34** was performed with a 30 min pre-incubation with 1 mM glutathione (which is comparable to levels of biological thiols), followed by a 30 min incubation with $3CL^{pro}$. As expected, the activity of the **34** was reduced, possessing an IC_{50} value of 13.6 ± 2.8 μM; however, this represents only ≈2-fold loss of activity. Following this, **34** was again pre-incubated for 30 min with 1 mM glutathione followed by a 240 min incubation with $3CL^{pro}$. Interestingly, the inhibition by compound **34** with this extended incubation time showed an IC_{50} value of 9.1 ± 1.8 μM, which is only slightly changed in comparison to the standard assay without addition of glutathione (Table 1). By comparison, the activity of the anticancer drug cisplatin is also reduced in the presence of glutathione,[52] and hence the reduced reactivity here is both expected and not an insurmountable impediment to further drug development.

Compound **34** was further investigated using a thermal shift assay as an orthogonal technique for evidence of enzyme binding. Compound **34** was incubated with $3CL^{pro}$ for 30 min at 37 °C and the melting temperature of the enzyme measured. While 4,4′-diamino-2,2′-bipyridine and the metal complex pentacarbonylchlororhenium showed only a negligible effect ($\Delta T = 0.2 \pm 0.4$), incubation with **34** gave a slight increase in the melting temperature of $3CL^{pro}$ ($\Delta T = 2.4 \pm 0.6$), indicative of inhibitor binding. Interestingly, the change in melting temperature was found to be in the same range as for the known inhibitor GC376 ($\Delta T = 3.1 \pm 0.5$).[53] The binding to $3CL^{pro}$ was further investigated by UV/Vis absorption spectroscopy (Figure S20). Compound **34** and $3CL^{pro}$ were combined and their absorption properties monitored every 2 min for 120 min. While no changes in the absorption spectra for **34** and $3CL^{pro}$ alone were observed under these conditions, the combined mixture of both showed changes. Within 30 min, an asymptotic absorption pattern was reached which showed no further changes after 60 min, suggestive of inhibitor binding (Figure S20).

As a means to characterize the binding affinity of the metal complex to the enzyme independently of intermediates, the ratio of the second reaction rate constant (k_2) in dependence of inhibition constant (K_i) was determined according to previously published procedures.[54] Lead compound **34** was incubated with $3CL^{pro}$ and the activity of the enzyme was monitored in a time-dependent manner. The metal complex was found to slowly bind to $3CL^{pro}$ with a ratio of k_2/K_i of 127 $M^{-1}s^{-1}$, which is two orders of magnitudes slower than the organic, covalent inhibitor GC376.[54] GC376 is a more potent inhibitor ($IC_{50} = 0.19 \pm 0.04$ μM) than **34**, which is consistent with difference in aforementioned k_2/K_i values. In addition, as found with compound **22**, incubation of compound **34** with $3CL^{pro}$ produced in an adduct that could be identified by mass spectrometry (see above). As expected, the deconvoluted mass peak of $3CL^{pro}$ shifted to 34255 (Figure S21) corresponding to a single attached Re^{I} tricarbonyl complex **34** (m/z 457).

Covalent $3CL^{pro}$ inhibitors could also bind and inhibit cathepsins, especially cathepsin B, resulting in undesired side reactions and off-target effects.[55] Inhibition of cathepsins is particularly relevant because they are found in the respiratory system, where SARS-CoV-2 would infect.[56] To investigate this potential shortcoming, cathepsin B was incubated with **34** for 2 h followed by analysis by mass spectrometry. While matrix-assisted laser ionization-time of flight mass spectrometry (MALDI-TOF-MS) identified the covalent adduct of **34** with $3CL^{pro}$ (Figure S22), no adduct formation was observed between **34** and cathepsin B (Figure S23), indicative of some selectivity of **34** towards $3CL^{pro}$ over this cysteine protease. To further evaluate selectivity, the activity of **34** against the human serine protease dipeptidyl peptidase-4 (DPP4), the aspartate protease beta-secretase 1 (BACE1) and cysteine protease cathepsin B was measured in an inhibition assay (Figure 6). Encouragingly, compound **34** did not show meas-

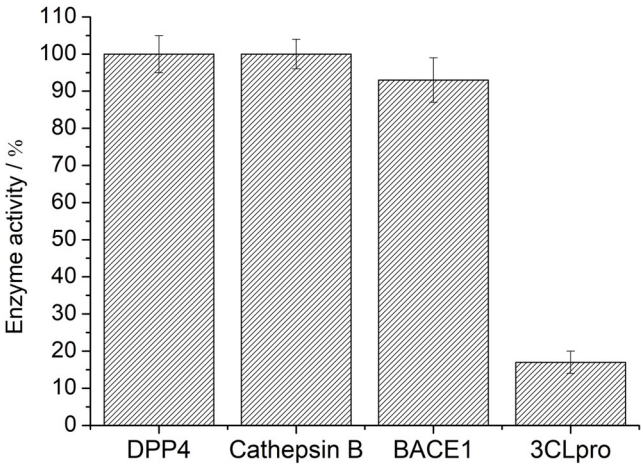

Figure 6. Enzymatic activity of the lead compound **34** at a concentration of 50 μM towards serine protease DPP4, aspartate protease BACE1, cysteine protease cathepsin B, and cysteine protease $3CL^{pro}$.

urable activity (IC_{50} value $>100\,\mu M$) towards DPP4 and cathepsin B, and showed only weak inhibition of BACE1 (IC_{50} value $= 89.2 \pm 5.7\,\mu M$). These preliminary studies indicate that selective inhibition of $3CL^{pro}$ can be achieved over several human proteases.

Conclusion

In summary, the synthesis and biophysical evaluation of Re^{I} tricarbonyl complexes as inhibitors of the SARS-CoV-2 main protease $3CL^{pro}$ has been achieved. A series of Re^{I} complexes with chloride and water as capping ligands and differently substituted 2,2′-bipyridine ligands were prepared. While the coordinated chloride was only slowly released, the aqua complex **22** showed reactivity towards amino acids within one hour. Mass spectrometry experiments verified the coordinate covalent binding of a single Re^{I} tricarbonyl complex to $3CL^{pro}$. Using an enzymatic assay against $3CL^{pro}$, several complexes were found to be active, with IC_{50} values of $<10\,\mu M$. Preliminary investigations show selectivity against human proteases. These results suggest that Re^{I} tricarbonyl complexes can serve as a starting scaffold for the development of potent, selective SARS-CoV-2 inhibitors.

Acknowledgements

The authors acknowledge the help of Ryjul W. Stokes with the measurement of NMR spectra and Dr. Yongxuan Su (UCSD, Molecular Mass Spectrometry Facility) with mass spectrometry. M.K. is supported by the Department of Defense (DoD) through the National Defense Science and Engineering Graduate (NDSEG) Fellowship Program is the recipient of an Achievement Rewards for College Scientists (ARCS) Foundation Fellowship. This work was supported by a grant from the National Institutes of Health (R21 AI138934).

Conflict of interest

The authors declare no conflict of interest.

Keywords: antiviral agents · bioinorganic chemistry · medicinal inorganic chemistry · protease inhibitor · SARS-CoV-2

[1] https://coronavirus.jhu.edu/map.html, last accessed 20.01.2021.
[2] C. M. Chu, V. C. C. Cheng, I. F. N. Hung, M. M. L. Wong, K. H. Chan, K. S. Chan, R. Y. T. Kao, L. L. M. Poon, C. L. P. Wong, Y. Guan, J. S. M. Peiris, K. Y. Yuen, *Thorax* **2004**, *59*, 252 – 256.
[3] I. L. Lu, N. Mahindroo, P.-H. Liang, Y.-H. Peng, C.-J. Kuo, K.-C. Tsai, H.-P. Hsieh, Y.-S. Chao, S.-Y. Wu, *J. Med. Chem.* **2006**, *49*, 5154 – 5161.
[4] A. E. Gorbalenya, A. P. Donchenko, V. M. Blinov, E. V. Koonin, *FEBS Lett.* **1989**, *243*, 103 – 114.
[5] Y. Chen, Q. Liu, D. Guo, *J. Med. Virol.* **2020**, *92*, 418 – 423.
[6] M.-H. Lin, D. C. Moses, C.-H. Hsieh, S.-C. Cheng, Y.-H. Chen, C.-Y. Sun, C.-Y. Chou, *Antiviral Res.* **2018**, *150*, 155 – 163.
[7] M. Gil-Moles, U. Basu, R. Büssing, H. Hoffmeister, S. Türck, A. Varchmin, I. Ott, *Chem. Eur. J.* **2020**, *26*, 15140 – 15144.
[8] T. Marzo, L. Messori, *ACS Med. Chem. Lett.* **2020**, *11*, 1067 – 1068.
[9] J. F.-W. Chan, Y. Yao, M.-L. Yeung, W. Deng, L. Bao, L. Jia, F. Li, C. Xiao, H. Gao, P. Yu, J.-P. Cai, H. Chu, J. Zhou, H. Chen, C. Qin, K.-Y. Yuen, *J. Infect. Dis.* **2015**, *212*, 1904 – 1913.
[10] A. C. Galasiti Kankanamalage, Y. Kim, V. C. Damalanka, A. D. Rathnayake, A. R. Fehr, N. Mehzabeen, K. P. Battaile, S. Lovell, G. H. Lushington, S. Perlman, K.-O. Chang, W. C. Groutas, *Eur. J. Med. Chem.* **2018**, *150*, 334 – 346.
[11] K. Karypidou, S. R. Ribone, M. A. Quevedo, L. Persoons, C. Pannecouque, C. Helsen, F. Claessens, W. Dehaen, *Bioorg. Med. Chem. Lett.* **2018**, *28*, 3472 – 3476.
[12] R.-J. Wu, K.-X. Zhou, H. Yang, G.-Q. Song, Y.-H. Li, J.-X. Fu, X. Zhang, S.-J. Yu, L.-Z. Wang, L.-X. Xiong, C.-W. Niu, F.-H. Song, H. Yang, J.-G. Wang, *Eur. J. Med. Chem.* **2019**, *167*, 472 – 484.
[13] L. Zhang, D. Lin, X. Sun, U. Curth, C. Drosten, L. Sauerhering, S. Becker, K. Rox, R. Hilgenfeld, *Science* **2020**, *368*, 409 – 412.
[14] W. Vuong, M. B. Khan, C. Fischer, E. Arutyunova, T. Lamer, J. Shields, H. A. Saffran, R. T. McKay, M. J. van Belkum, M. A. Joyce, H. S. Young, D. L. Tyrrell, J. C. Vederas, M. J. Lemieux, *Nat. Commun.* **2020**, *11*, 4282.
[15] Z. Jin, X. Du, Y. Xu, Y. Deng, M. Liu, Y. Zhao, B. Zhang, X. Li, L. Zhang, C. Peng, Y. Duan, J. Yu, L. Wang, K. Yang, F. Liu, R. Jiang, X. Yang, T. You, X. Liu, X. Yang, F. Bai, H. Liu, X. Liu, L. W. Guddat, W. Xu, G. Xiao, C. Qin, Z. Shi, H. Jiang, Z. Rao, H. Yang, *Nature* **2020**, *582*, 289 – 293.
[16] T. Pillaiyar, M. Manickam, V. Namasivayam, Y. Hayashi, S.-H. Jung, *J. Med. Chem.* **2016**, *59*, 6595 – 6628.
[17] B. A. Malcolm, C. Lowe, S. Shechosky, R. T. McKay, C. C. Yang, V. J. Shah, R. J. Simon, J. C. Vederas, D. V. Smith, *Biochemistry* **1995**, *34*, 8172 – 8179.
[18] H. Bregman, P. J. Carroll, E. Meggers, *J. Am. Chem. Soc.* **2006**, *128*, 877 – 884.
[19] L. Feng, Y. Geisselbrecht, S. Blanck, A. Wilbuer, G. E. Atilla-Gokcumen, P. Filippakopoulos, K. Kräling, M. A. Celik, K. Harms, J. Maksimoska, R. Marmorstein, G. Frenking, S. Knapp, L.-O. Essen, E. Meggers, *J. Am. Chem. Soc.* **2011**, *133*, 5976 – 5986.
[20] C. N. Morrison, K. E. Prosser, R. W. Stokes, A. Cordes, N. Metzler-Nolte, S. M. Cohen, *Chem. Sci.* **2020**, *11*, 1216 – 1225.
[21] E. J. Anthony, E. M. Bolitho, H. E. Bridgewater, O. W. L. Carter, J. M. Donnelly, C. Imberti, E. C. Lant, F. Lermyte, R. J. Needham, M. Palau, P. J. Sadler, H. Shi, F.-X. Wang, W.-Y. Zhang, Z. Zhang, *Chem. Sci.* **2020**, https://doi.org/10.1039/D1030SC04082G.
[22] J. Karges, *ChemBioChem* **2020**, *21*, 3044 – 3046.
[23] I. Romero-Canelón, P. J. Sadler, *Proc. Natl. Acad. Sci. USA* **2015**, *112*, 4187 – 4188.
[24] C. G. Hartinger, N. Metzler-Nolte, P. J. Dyson, *Organometallics* **2012**, *31*, 5677 – 5685.
[25] A. K. Ghosh, I. Samanta, A. Mondal, W. R. Liu, *ChemMedChem* **2019**, *14*, 889 – 906.
[26] J. Singh, R. C. Petter, T. A. Baillie, A. Whitty, *Nat. Rev. Drug Discovery* **2011**, *10*, 307 – 317.
[27] M. Rausch, P. J. Dyson, P. Nowak-Sliwinska, *Adv. Ther.* **2019**, *2*, 1900042.
[28] S. P. Fricker, R. M. Mosi, B. R. Cameron, I. Baird, Y. Zhu, V. Anastassov, J. Cox, P. S. Doyle, E. Hansell, G. Lau, J. Langille, M. Olsen, L. Qin, R. Skerlj, R. S. Y. Wong, Z. Santucci, J. H. McKerrow, *J. Inorg. Biochem.* **2008**, *102*, 1839 – 1845.
[29] S. P. Fricker, *Metallomics* **2010**, *2*, 366 – 377.
[30] K. P. Kepp, *Inorg. Chem.* **2016**, *55*, 9461 – 9470.
[31] W. M. Haynes, *CRC Handbook of Chemistry and Physics*, CRC, Boca Raton, **2014**.

[32] S. C. Marker, A. P. King, S. Granja, B. Vaughn, J. J. Woods, E. Boros, J. J. Wilson, *Inorg. Chem.* **2020**, *59*, 10285 – 10303.
[33] C. C. Konkankit, A. P. King, K. M. Knopf, T. L. Southard, J. J. Wilson, *ACS Med. Chem. Lett.* **2019**, *10*, 822 – 827.
[34] C. Philippe, D. Didier, V. Veena, *Curr. Pharm. Des.* **2019**, *25*, 3306 – 3322.
[35] M. S. Capper, H. Packman, M. Rehkämper, *ChemBioChem* **2020**, *21*, 2111 – 2115.
[36] L. J. Raszeja, D. Siegmund, A. L. Cordes, J. Güldenhaupt, K. Gerwert, S. Hahn, N. Metzler-Nolte, *Chem. Commun.* **2017**, *53*, 905 – 908.
[37] M. Muñoz-Osses, F. Godoy, A. Fierro, A. Gómez, N. Metzler-Nolte, *Dalton Trans.* **2018**, *47*, 1233 – 1242.
[38] P. Kurz, B. Probst, B. Spingler, R. Alberto, *Eur. J. Inorg. Chem.* **2006**, 2966 – 2974.
[39] M. Towrie, A. W. Parker, K. L. Ronayne, K. F. Bowes, J. M. Cole, P. R. Raithby, J. E. Warren, *Appl. Spectrosc.* **2009**, *63*, 57 – 65.
[40] J. M. Smieja, C. P. Kubiak, *Inorg. Chem.* **2010**, *49*, 9283 – 9289.
[41] B. J. Coe, S. P. Foxon, R. A. Pilkington, S. Sánchez, D. Whittaker, K. Clays, N. Van Steerteghem, B. S. Brunschwig, *Organometallics* **2016**, *35*, 3014 – 3024.
[42] M. L. Clark, B. Rudshteyn, A. Ge, S. A. Chabolla, C. W. Machan, B. T. Psciuk, J. Song, G. Canzi, T. Lian, V. S. Batista, C. P. Kubiak, *J. Phys. Chem. C* **2016**, *120*, 1657 – 1665.
[43] G. F. Manbeck, J. T. Muckerman, D. J. Szalda, Y. Himeda, E. Fujita, *J. Phys. Chem. B* **2015**, *119*, 7457 – 7466.
[44] G. A. Bhat, A. Z. Rashad, T. M. Folsom, D. J. Darensbourg, *Organometallics* **2020**, *39*, 1612 – 1618.
[45] D. A. Popov, J. M. Luna, N. M. Orchanian, R. Haiges, C. A. Downes, S. C. Marinescu, *Dalton Trans.* **2018**, *47*, 17450 – 17460.
[46] S. Lense, N. A. Piro, S. W. Kassel, A. Wildish, B. Jeffery, *Acta Crystallogr. Sect. E* **2016**, *72*, 1201 – 1205.
[47] K. M. Knopf, B. L. Murphy, S. N. MacMillan, J. M. Baskin, M. P. Barr, E. Boros, J. J. Wilson, *J. Am. Chem. Soc.* **2017**, *139*, 14302 – 14314.
[48] S. Keller, Y. C. Ong, Y. Lin, K. Cariou, G. Gasser, *J. Organomet. Chem.* **2020**, *906*, 121059.
[49] M. S. Capper, A. Enriquez Garcia, N. Macia, B. Lai, J.-B. Lin, M. Nomura, A. Alihosseinzadeh, S. Ponnurangam, B. Heyne, C. S. Shemanko, F. Jalilehvand, *J. Biol. Inorg. Chem.* **2020**, *25*, 759 – 776.
[50] J. Lecina, Ò. Palacios, S. Atrian, M. Capdevila, J. Suades, *J. Biol. Inorg. Chem.* **2015**, *20*, 465 – 474.
[51] T. R. Steel, C. G. Hartinger, *Metallomics* **2020**, *12*, 1627 – 1636.
[52] H. H. W. Chen, M. T. Kuo, *Met.-Based Drugs* **2010**, *2010*, 430939.
[53] Y. Kim, H. Liu, A. C. Galasiti Kankanamalage, S. Weerasekara, D. H. Hua, W. C. Groutas, K.-O. Chang, N. C. Pedersen, *PLOS Pathog.* **2016**, *12*, e1005531.
[54] C. Ma, M. D. Sacco, B. Hurst, J. A. Townsend, Y. Hu, T. Szeto, X. Zhang, B. Tarbet, M. T. Marty, Y. Chen, J. Wang, *Cell Res.* **2020**, *30*, 678 – 692.
[55] K. Steuten, H. Kim, J. C. Widen, B. M. Babin, O. Onguka, S. Lovell, O. Bolgi, B. Cerikan, M. Cortese, R. K. Muir, J. M. Bennett, R. Geiss-Friedlander, C. Peters, R. Bartenschlager, M. Bogyo, *BioRxiv* **2020**, https://doi.org/10.1101/2020.11.21.392753.
[56] S. Lukassen, R. L. Chua, T. Trefzer, N. C. Kahn, M. A. Schneider, T. Muley, H. Winter, M. Meister, C. Veith, A. W. Boots, B. P. Hennig, M. Kreuter, C. Conrad, R. Eils, *EMBO J.* **2020**, *39*, e105114.
[57] Deposition Numbers 2026146, 2026147, 2026148, 2026149, 2026150, 2026151, 2026152, 2026153, 2026154, 2026155, 2026156 and 2026157 (for **3**, **7**, **8**, **11**, **13**, **14**, **15**, **19**, **20**, **22**, **37**, and **42**, respectively) contain the supplementary crystallographic data for this paper. These data are provided free of charge by the joint Cambridge Crystallographic Data Centre and Fachinformationszentrum Karlsruhe Access Structures service www.ccdc.cam.ac.uk/structures.

Manuscript received: December 17, 2020
Revised manuscript received: February 10, 2021
Accepted manuscript online: February 19, 2021
Version of record online: March 26, 2021

